Bispecific small molecule–antibody conjugate targeting prostate cancer

Chan Hyuk Kim[a,1], Jun Y. Axup[b,c], Brian R. Lawson[a,d], Hwayoung Yun[b,c], Virginie Tardif[d], Sei Hyun Choi[b,c], Quan Zhou[b,c], Anna Dubrovska[b,c], Sandra L. Biroc[e], Robin Marsden[e], Jason Pinstaff[e], Vaughn V. Smider[f], and Peter G. Schultz[a,b,c,1]

Departments of [b]Chemistry, [d]Immunology and Microbial Science, and [f]Molecular Biology and [c]The Skaggs Institute for Chemical Biology, The Scripps Research Institute, La Jolla, CA 92037; [a]California Institute for Biomedical Research, La Jolla, CA 92037; and [e]Ambrx, Inc., La Jolla, CA 92037

Bispecific antibodies, which simultaneously target CD3 on T cells and tumor-associated antigens to recruit cytotoxic T cells to cancer cells, are a promising new approach to the treatment of hormone-refractory prostate cancer. Here we report a site-specific, semisynthetic method for the production of bispecific antibody-like therapeutics in which a derivative of the prostate-specific membrane antigen-binding small molecule DUPA was selectively conjugated to a mutant αCD3 Fab containing the unnatural amino acid, p-acetylphenylalanine, at a defined site. Homogeneous conjugates were generated in excellent yields and had good solubility. The efficacy of the conjugate was optimized by modifying the linker structure, relative binding orientation, and stoichiometry of the ligand. The optimized conjugate showed potent and selective in vitro activity (EC$_{50}$ ∼100 pM), good serum half-life, and potent in vivo activity in prophylactic and treatment xenograft mouse models. This semisynthetic approach is likely to be applicable to the generation of additional bispecific agents using drug-like ligands selective for other cell-surface receptors.

antibody engineering | immunotherapy

Prostate cancer is the second most common cancer in men in the United States with more than 28,000 prostate cancer-specific deaths and 240,000 newly diagnosed patients in 2012 (1). Although surgery, radiation, and antiandrogen therapies are increasingly effective, the disease often progresses to hormone-refractory prostate cancer and metastasis resulting in a very poor prognosis (1–2 y of median overall survival after tumor relapse) (2, 3). Recently, there has been increased interest in the use of antibody–drug conjugates to deliver cytotoxic drugs selectively to prostate cancer cells (4). Immunotherapeutics that target tumor-associated antigens such as prostate-specific antigen, prostate acid phosphatase, and prostate-specific membrane antigen (PSMA) provide an alternative strategy to kill prostate cancer cells selectively while minimizing the collateral damage to other normal tissues (5–9). Bispecific antibodies that bind both T-cell surface antigen (CD3) and tumor-associated antigens can recruit endogenous cytotoxic T cells to cancer cells, resulting in specific T-cell activation and cancer cell death (10). Bispecific antibodies also may kill heterogeneous tumor or quiescent cancer stem cells through a bystander effect, as well as drug-resistant tumors with up-regulated drug pumps (11, 12). Indeed two bispecific antibodies, catumaxomab (αEpCAM/αCD3) and blinatumomab (αCD19/αCD3), have shown impressive results in the treatment of malignant ascites and refractory acute lymphoblastic leukemia, respectively (13, 14).

Although bispecific antibodies are generating a great deal of interest, current technologies for their production still face challenges. For example, recombinant single-chain variable fragment (scFv) formats can have poor physical properties and short plasma half-lives, and some hybrid IgG constructs show an immunogenic response because of the development of human anti-mouse antibodies or human anti-rat antibodies in patients (15). Alternatively, the generation of bispecific antibodies by semisynthetic methods, in which independently expressed

antibodies are chemically crosslinked, may provide a number of advantages compared with genetic methods. For example, unlike the fixed direction of N→C genetic fusions, semisynthetic methods allow more freedom to alter the orientation and distance of the two antigen-binding moieties of bispecific antibodies to optimize their efficacy. However, conventional chemical approaches that use lysine or cysteine chemistry tend to yield heterogeneous products which likely differ in their ability to accommodate productive geometries for the formation of immunological synapses and/or have reduced stability or half-life in vivo (16). Previously, we reported a semisynthetic method in which an unnatural amino acid with orthogonal chemical reactivity was introduced genetically at a desired site in antibody fragments (Fabs) and then derivatized site-specifically with heterobifunctional cross-linkers to generate homogeneous, chemically defined bispecific antibodies (17). In an effort to explore further semisynthetic approaches to generate bispecific therapeutics, here we report a method of producing hybrid antibody–small molecule conjugates with activities similar to those of bispecific antibodies. Specifically, a synthetic small molecule ligand, 2-[3-(1, 3-dicarboxy propyl)-ureido] pentanedioic acid (DUPA), that selectively binds PSMA (18) was used as the cancer-targeting moiety and was conjugated to an αCD3 Fab. The ability to incorporate the unnatural amino acid selectively at defined sites allowed us to optimize the conjugation site and stoichiometry of the antibody–small molecule conjugate. Our lead molecule showed potent in vitro cytotoxicity (EC$_{50}$ ∼100 pM) against PSMA$^+$ prostate cancer cells in the presence of human peripheral blood mononuclear cells (hPBMCs), had significantly

Significance

We have developed a semisynthetic method for the production of bispecific antibody-like therapeutics consisting of a small molecule targeting moiety conjugated to an antibody. A highly selective prostate-specific membrane antigen-binding ligand was site specifically conjugated to a mutant α cluster of differentiation 3 (αCD3) Fab containing an unnatural amino acid with orthogonal chemical reactivity. The optimized conjugate showed potent in vitro activity, good serum half-life, and potent in vivo activity in prostate cancer xenograft mouse models. This semisynthetic approach is likely to be applicable to the generation of additional bispecific agents using drug-like ligands selective for other cell-surface receptors.

APPLIED BIOLOGICAL SCIENCES

improved pharmacokinetics compared with the unconjugated Fab, and was efficacious in mouse xenograft models.

Results and Discussion

Design and Synthesis of Bispecific Antibody–Small Molecule Conjugates. Homogeneous but highly restricted expression of tumor-associated antigens is critical to the success of targeted immunotherapies. PSMA, also known as glutamate carboxypeptidase II or N-acetyl-L-aspartyl-L-glutamate peptidase I, is an excellent cell-surface target for prostate cancer because its expression is up-regulated throughout all stages of prostate cancer progression and is highly restricted to prostate cells, with very low levels of expression detectable in other tissues (19). Indeed, several αPSMA monoclonal antibodies have been used as vehicles for the targeted delivery of cytotoxic agents including radioactive isotopes, small molecules, and protein toxins (4, 20, 21). A series of small molecule PSMA inhibitors with high affinity (in the low nanomolar range) and selectivity also have been explored for selective lysis or imaging of PSMA⁺ prostate cancer cells (18, 22, 23). Because of their small size, such small molecule-based targeting agents (peptides, vitamins, and substrate analogs) have better tumor penetration than antibodies (24). They also are amenable to extensive chemical modification and can be derivatized easily with other molecules, including proteins. Among several small molecule inhibitors of PSMA, we chose an urea-based inhibitor, DUPA, because of its high affinity ($K_i = 8$ nM) and selectivity for PSMA. DUPA was modified with a short (P-Tet; **1**) and a longer (P-Und; **2**) ethylene glycol linker to determine the best chain length to bind the deep binding pocket of PSMA. Also, based on a previous report of a second arene-binding motif near the active site of PSMA, we synthesized two additional linkers, P-Phthal (**3**) and P-DNP (**4**), containing 1,4-dicarboxylic and 1,3-dinitro substituted phenyl moieties, respectively, in an effort to increase binding affinity further (Fig.

1A) (25). All the DUPA–linker conjugates have aminooxy groups at their termini that form a stable oxime bond with ketone group. To evaluate their activity, the inhibition constant (K_i) of each compound was measured using purified PSMA enzyme (R&D Systems) and its substrate, N-acetylaspartylglutamic acid. This analysis revealed that the incorporation of an electron-deficient aromatic group in the linker (P-DNP; **4**) resulted in a 100-fold increased inhibitory activity ($K_i = 0.087$ nM) relative to free DUPA. The shorter unsubstituted ethylene glycol linker P-Tet (**1**; $K_i = 0.90$ nM) bound more tightly than P-Phthal (**3**; $K_i = 2.5$ nM), whereas P-Und (**2**; $K_i = 17$ nM) showed significantly reduced activity (Fig. S1).

To conjugate the DUPA–linker moiety to an anti-CD3 antibody, we expressed a mutant αCD3 Fab, UCHT1, in which the unnatural amino acid, p-acetyl phenylalanine (pAcF) was substituted for the heavy-chain residue K138 (HC K138) (26, 27). A humanized αCD3 antibody, UCHT1 reduces immunogenicity, and its ability to retarget cytotoxic T cells efficiently has been demonstrated in a bispecific antibody format (17, 28). A ketone functional group in pAcF ensures selective modification of the UCHT1 Fab with aminooxy-derivatized DUPA. The position of the unnatural amino acid was chosen based on the known crystal structure of an antibody in the same class (Herceptin Fab, IgG1 κ-light chain) (29). HC K138 is distal to the antigen-binding site, and is surface exposed to ensure efficient conjugation with small molecules. Specifically, a plasmid (pBAD_UCHT1_HC-138X, X = TAG) harboring the light- and heavy-chain genes of the antibody following an stII signal sequence was cotransformed into *Escherichia coli* DH10B strain with a plasmid (pULTRA_pAcF) harboring an orthogonal *Methanocaldococcus jannaschii* tRNA/tyrosyl-tRNA synthetase (Mj-TyrRS) pair, which was evolved to incorporate pAcF selectively in response to the amber nonsense codon (30). The expression levels of the mutant Fab (∼2 mg/L in a shaker flask)
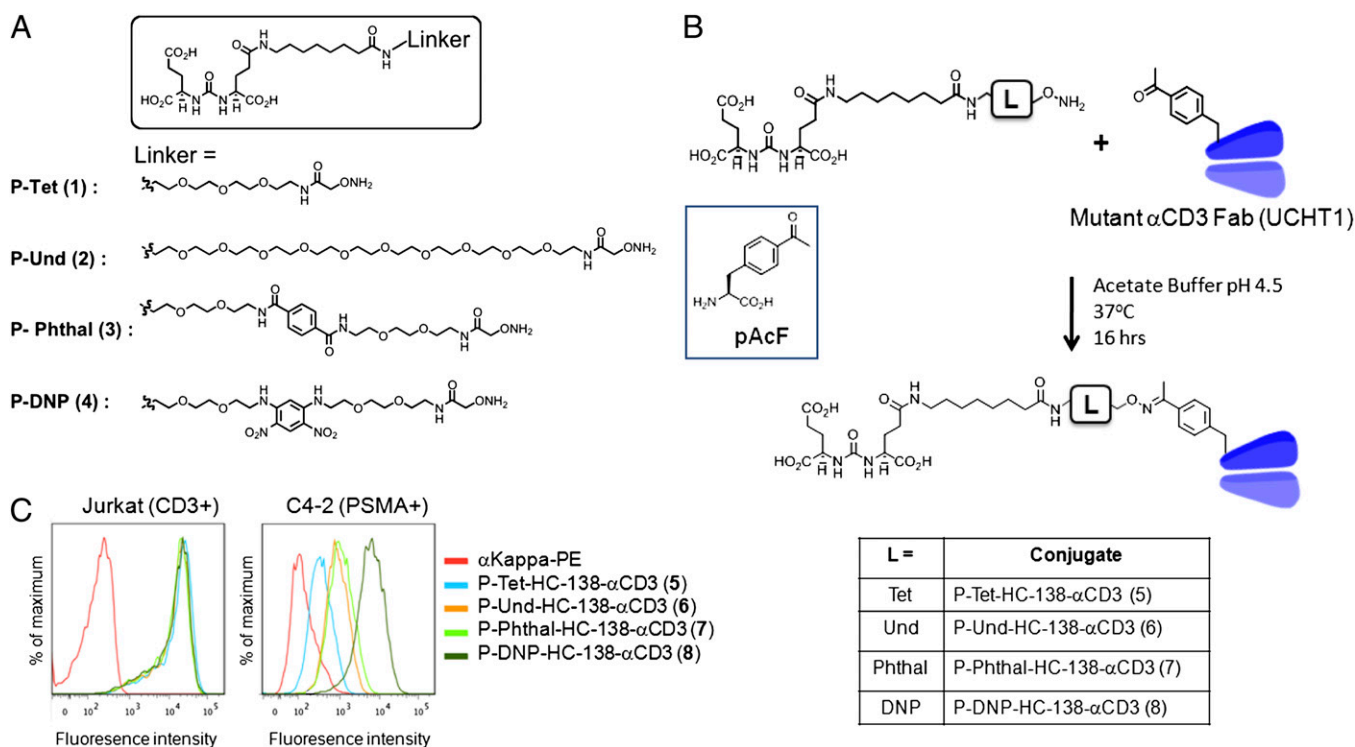
Fig. 1. (A) Structure of DUPA modified with short ethylene glycol (Tet, **1**), long ethylene glycol (Und, **2**), Phthal (**3**), and DNP (**4**) linkers with a terminal aminooxy group. (B) Structure of p-acetylphenylalnine (pAcF) and oxime ligation of pAcF containing αCD3 Fab with P–linkers. (C) FACS of the P-αCD3 conjugates (100 nM) on Jurkat (CD3⁺) and C4-2 (PSMA⁺) cell lines. Different P–linkers are conjugated to the same residue (HC-138) of the αCD3 Fab.

Kim et al.

were comparable to those of the wild-type Fab after purification using affinity chromatography (Protein G; GE Healthcare). The purified mutant anti-CD3 Fab (2 mg/mL) was conjugated to each DUPA–linker compound (100-fold molar excess) by selective formation of a stable oxime bond under somewhat acidic conditions (100 mM NaOAc, pH 4.5); liquid chromatography-mass spectrometry (LC-MS) showed >95% coupling efficiency within 24 h. The excess DUPA–linker compounds were removed by size-exclusion methods yielding highly homogeneous conjugation products as determined by SDS/PAGE and LC-MS characterization (*SI Materials and Methods*). No protein aggregation was observed during the reaction and purification steps even at higher concentrations (>10 mg/mL), indicating that conjugation of DUPA–linkers did not alter the solubility of the Fab significantly. The same procedure was used to prepare the antibody conjugates P-Tet-HC-138-αCD3 (**5**), P-Und-HC-138-αCD3 (**6**), P-Phthal-HC-138-αCD3 (**7**), and P-DNP-HC-138-αCD3 (**8**) (Fig. 1*B*) in comparable yields and purity.

We next tested the binding affinity of the conjugates (100 nM) to CD3$^+$ Jurkat cells and PSMA$^+$ C4-2 cells. All conjugates had similar affinity for Jurkat cells, demonstrating that binding of the αCD3 Fab is not affected by small molecule conjugation (Fig.

1*C*). In contrast, the assay with C4-2 cells revealed different binding affinities for the different conjugates, as expected based on the different affinities of the DUPA–linker moieties. Interestingly, P-Und-HC-138-αCD3 (**6**), which contains the linker with lowest affinity in the previous assay, bound more tightly than P-Tet-HC-138-αCD3 (**5**), likely because of the deep ligand-binding pocket of PSMA (31). As expected, P-DNP-HC-138-αCD3 (**8**) again showed the highest affinity, followed by P-Phthal-HC-138-αCD3 (**7**) (Fig. 1*C*). These results underscore the value of optimizing conjugate affinity by modifications to the small molecule component of these hybrid bispecifics.

Effect of Conjugation Site and Stoichiometry. The recombinant incorporation of unnatural amino acids not only allows us to modify antibodies site specifically; it also allows the facile generation and evaluation of various antibody conjugates with different relative geometries (Fig. 2*A*) (32), which may affect the formation of an optimal pseudoimmunological synapse. Therefore, in addition to HC K138X, we chose three additional sites [light-chain (LC) T109X, LC S202X, and HC A123X], all of which are distal to the antigen-binding site, for conjugation of DUPA–linkers based on the crystal structure (Fig. 2*A*), and expressed mutant antibodies
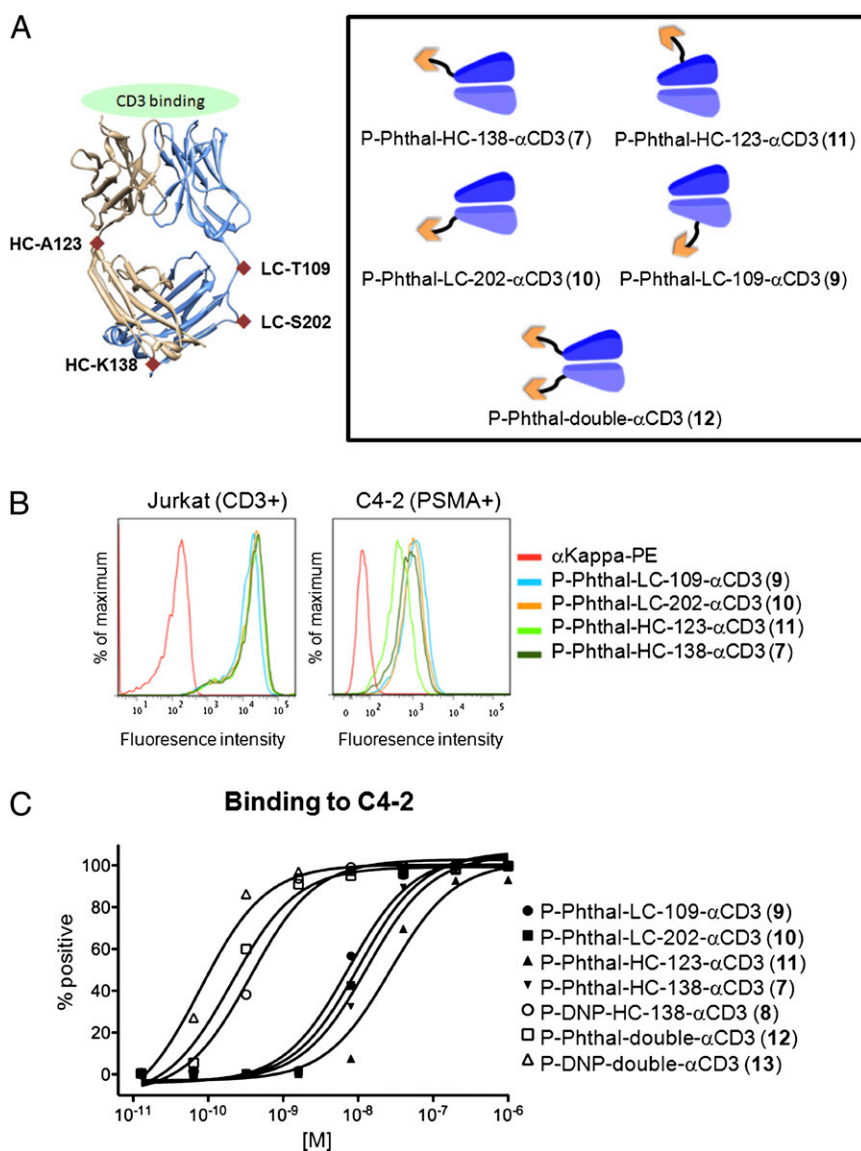
Fig. 2. (*A*) Sites of mutation in αCD3 Fab for the single and double conjugates. Each mutant conjugate results in a distinct orientation for PSMA binding relative to CD3 binding. The double-αCD3 conjugate (HC-K138/LC-S202) increases avidity to homodimeric PSMA. (*B*) FACS of the P-αCD3 (100 nM) conjugates on Jurkat (CD3$^+$) and C4-2 (PSMA$^+$) cell lines. P-Phthal is conjugated to different positions of the αCD3 Fab. (*C*) FACS analysis of the binding of different mono- and bivalent P-αCD3 conjugates to C4-2 cells at various concentrations.

Kim et al.

with pAcF, as described above, in comparable yields. For comparison, each mutant αCD3 Fab was conjugated to P-Phthal (**3**) to afford P-Phthal-LC-109-αCD3 (**9**), P-Phthal-LC-202-αCD3 (**10**), and P-Phthal-HC-123-αCD3 (**11**). The resulting conjugates were tested for binding to CD3 and PSMA by flow cytometry. Because each conjugation site is distal from the antigen-binding site of the anti-CD3 antibody, they showed binding similar to $CD3^+$ Jurkat cells, as expected (Fig. 1C). Interestingly, however, when we repeated the binding assay with C4-2 cells, the HC A123 conjugate showed decreased binding to C4-2 cells, whereas the other three conjugates (LC T109 and S202 and HC K138) bound C4-2 cells with similar affinity. This result clearly shows that the conjugation site affects ligand binding (Fig. 2B).

Previous reports indicate that a higher antigen affinity correlates to enhanced cytotoxicity of bispecific antibodies (33). Therefore, we also conjugated two DUPA ligands to each αCD3 Fab so that the bivalent ligand can bind the PSMA homodimer with high avidity (34). To synthesize a bivalent Fab, we introduced TAG codons at two different positions (LC S202 and HC K138), and the double mutant was expressed and purified as described above. Notably, the expression levels were comparable to those of other single mutants and the wild-type antibody that were previously expressed. The double-mutant antibody was conjugated with P-Phthal (**3**) or P-DNP (**4**) as described above. LC-MS analysis revealed that the reaction was complete within 48 h, yielding the bivalent conjugates, P-Phthal-double-αCD3 (**12**) and P-DNP-double-αCD3 (**13**). After purification, the structures were confirmed by SDS/PAGE and LC-MS (*SI Materials and Methods*). Binding of the bivalent conjugates to C4-2 cells then was assessed (together with monovalent conjugates) using high-throughput flow cytometry (Fig. 2C). A significant improvement was observed in binding affinity (>60-fold) for the bivalent P-Phthal-double-αCD3 (**12**) compared with the monovalent P-Phthal-HC-138-αCD3 (**7**). Interestingly, P-DNP-double-αCD3 (**13**) did not show significant improvement over its monovalent equivalent P-DNP-HC-138-αCD3 (**8**), which already had high affinity. The enhanced binding affinity of P-Phthal-double-αCD3 (**12**) was particularly encouraging because, despite the high affinity of the DNP group, its known high immunogenicity might limit its use in vivo (35).

In Vitro Cytotoxicity of αPSMA/αCD3 Conjugates. We next compared the in vitro cytotoxicity of various αPSMA/αCD3 conjugates. Freshly purified hPBMCs were mixed with C4-2 ($PSMA^+$) cells at a 10:1 ratio (100,000 and 10,000 cells, respectively) and were incubated with each conjugate for 24 h. A 1:1 mixture of wild-type UCHT1 Fab and the DUPA–linker conjugate (P-DNP, **4**) was used as a negative control. Cytotoxicity was determined by measuring lactose dehydrogenase (LDH) released from lysed target cells (36). As shown in Fig. 3A, each of the conjugates, with the exception of P-Phthal-HC-123-αCD3 (**11**), which bound C4-2 cells poorly in the previous assay, showed dose-dependent cytotoxicity. P-Phthal-LC-109-αCD3 (**9**) showed reduced cytotoxicity (EC_{50} ~4.1 nM) compared with P-Phthal-LC-202-αCD3 (**10**) and P-Phthal-HC-138-αCD3 (**7**) (EC_{50} ~0.4 nM and ~0.5 nM, respectively), although all had similar affinities in the binding studies. Finally, P-Phthal-double-αCD3 (**12**) showed the highest cytotoxicity (EC_{50} ~0.1 nM) compared with the monovalent constructs. No cytotoxicity was observed even at the highest concentration measured with the unconjugated DUPA–linker and UCHT1 Fab mixtures. Taken together, these results imply that both the affinity and the geometry of the bispecific binding significantly affect cytotoxicity. Based on the binding and in vitro cytotoxicity assays, we chose P-Phthal-double-αCD3 (**12**) (hereafter referred to as "PSMA-targeting small molecule antibody conjugate," P-SMAC) for further characterization.

We confirmed the specificity of the P-SMAC molecule for PSMA-expressing cells in vitro using $PSMA^−$ DU145 cells in the
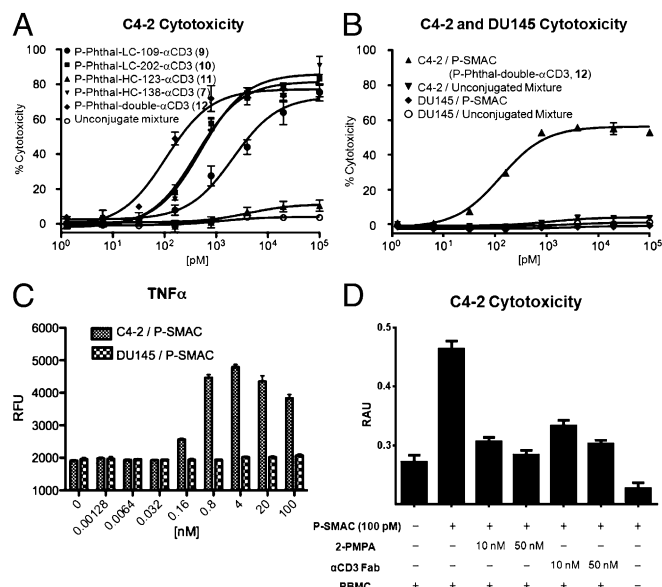
Fig. 3. In vitro cytotoxicity of αPSMA/αCD3 conjugates in the presence of freshly purified unactivated hPBMCs. (*A*) Conjugates show dose-dependent activity on $PSMA^+$ C4-2 cells with different EC_{50} values, whereas the unconjugated mixture shows no activity. (*B*) Conjugates have no effect on $PSMA^−$ DU-145 cells. Cytotoxicity was detected by LDH-release assay. (*C*) Proinflammatory cytokine TNF-α levels in the supernatant of the cytotoxicity assay. Dose-dependent TNF-α signals were detected by ELISA only in the presence of $PSMA^+$ C4-2 cells. RFU, relative fluorescence units. (*D*) Significantly reduced cytotoxicity of C4-2 cells was observed in the competition assay in the presence of either the competitive antagonist 2-phosphonomethyl pentanedioic acid (2-PMPA) or αCD3 Fab. No cytotoxicity was observed in the absence of hPBMCs. RAU, relative absorbance units.

same cytotoxicity assay. No cytotoxicity was observed with DU145 cells in the presence of hPBMCs, regardless of the conjugation status or concentrations of the constructs (Fig. 3B). Furthermore, a dose-dependent increase in TNF-α levels in the supernatant was observed only in the presence of C4-2 cells, indicating specific activation of T cells after the formation of a pseudoimmunological synapse between C4-2 and T cells (Fig. 3C) (37). The rosette morphology that is evident upon synapse formation was observed clearly only in the presence of the P-SMAC with C4-2 cells (Fig. S2). We also showed that the competitive inhibitors, 2-phosphonomethyl pentanedioic acid and αCD3 Fab, can inhibit the cytotoxicity of P-SMAC against C4-2 cells significantly, confirming that simultaneous binding to two antigens is crucial for the activity of the bispecific conjugate. Finally, P-SMAC itself showed no cytotoxicity against C4-2 cells in the absence of hPBMCs (Fig. 3D).

In Vivo PK and Antitumor Activity. We first evaluated the pharmacokinetics of the P-SMAC. Male Sprague–Dawley rats (Charles River Laboratories) were injected i.v. at time 0 with 1 and 5 mg/kg P-SMAC or 0.5 mg/kg of the unconjugated UCHT1 Fab. Blood was collected at regular intervals to 32 h and was processed to measure drug concentrations using a sandwich-ELISA (see *SI Materials and Methods* for the detailed procedure). Interestingly, the P-SMAC showed significantly improved circulating half-life (~5–6 h) compared with the unconjugated Fab (~1 h), perhaps because of the increased overall hydrophobicity of the Fab after conjugation (Fig. S3) (38, 39). Of note, P-SMAC has an improved serum half-life relative to small bispecific scFvs such as bispecific T-cell engagers, which have a half-life of ~2 h in humans, despite their similar molecular weight

(∼50,000 Da) (40, 41). The small size of the P-SMAC also may be advantageous for penetrating solid tumors (42).

We next established a mouse xenograft model to evaluate the in vivo efficacy of the P-SMAC. Immunodeficient NOD/SCID mice (from The Scripps Research Institute breeding colony) were s.c. injected with a mixture of 1×10^6 C4-2 cells and 2×10^6 hPBMCs in Matrigel (BD Bioscience). After 4 d, treatment was initiated by injecting 2 mg/kg of drug via the tail vein and was continued daily for 10 d ($n = 6$). In a control group, mice were injected with an unconjugated mixture of P-Phthal (**3**) and UCHT1 wild-type Fab, and in another control group mice were injected with vehicle alone ($n = 6$). Tumor growth was monitored by external caliper measurement. The two control groups showed tumor outgrowth approximately 2 wk after implantation. However, the treatment group did not develop any palpable tumors for up to 6 wk, at which time all the mice in the other two groups had to be euthanized because of the large tumor sizes (Fig. 4A).

Having demonstrated prophylactic efficacy with the P-SMAC, we next carried out a xenograft model in which we delayed treatment until we observed the formation of a palpable tumor. In this treatment study, we used NOD/SCID-γ mice (Jackson Laboratory), which are known to be more suitable for immune reconstitution with human-derived cells. On day zero, 1×10^6 C4-2 cells in Matrigel were s.c. injected, and after 3 d 20×10^6 hPBMCs were separately injected into the peritoneal cavity. This separate injection of hPBMCs allows further assessment of the capability of the P-SMAC to redirect T cells from the periphery to the site of tumor. Palpable solid tumors (∼200 mm³) were formed in mice approximately 2 wk after tumor implantation. Before starting treatment, ex vivo-expanded T cells (20×10^6 cells per mouse) from the same donor were i.p. injected in all groups, further supplementing the effector cell pool. Two days later, we started treatment via tail-vein injection with 1 mg/kg P-SMAC for 10 d ($n = 9$). Shortly after treatment was initiated, tumor shrinkage was observed in the P-SMAC group, whereas the vehicle group ($n = 8$) again showed rapid tumor outgrowth. After 10 d treatment was stopped, tumor growth was monitored for an additional 10 d, during which no significant tumor regrowth was observed in the treatment group. These results demonstrate that the P-SMAC is efficacious against established tumors in mice (Fig. 4B). During the experiment, no overt toxicity or body weight loss was observed in mice in any group (Fig. S4). Histology also confirmed the formation of solid tumors with high mitotic rates in mice from the control group, whereas only residual tumor cells with low mitotic rates were detected in the treatment group (Fig. S5).

Conclusion

The genetic incorporation of the unnatural amino acid pAcF, which is orthogonal to the canonical 20 amino acids in its chemical reactivity, makes it possible to generate antibody conjugates with medicinal chemistry-like control over structure. As a consequence, one can begin to optimize the efficacy of the conjugates by modifying the relative orientation and distance of the two antigen-binding sites in bispecific antibodies. We used this methodology to synthesize a PSMA-targeting small molecule–antibody conjugate (P-SMAC), which consists of a bivalent PSMA-binding molecule, DUPA, conjugated to the humanized αCD3 antibody Fab UCHT1. P-SMAC has potent (EC$_{50}$ ∼100 pM) and selective in vitro cytotoxic activity against the PSMA$^+$ prostate cancer cell line C4-2 in the presence of hPBMCs. P-SMAC also demonstrated good solubility and serum half-life and has potent in vivo antitumor activity in mouse xenograft models.

The use of pAcF offers a number of advantages for constructing these hybrid antibody conjugates. It can be incorporated at a large number of sites throughout the antibody [and at multiple sites (30)], affords excellent one-step conjugation yields, and results in a linkage that is very stable under physiological conditions. Indeed, we show that changes in conjugation site and linker structure can affect SMAC activity significantly. Recently, Rader and co-workers reported a site-specific method of antibody conjugation relying on selenocysteine (Sec) that is cotranslationally introduced into antibody molecules (43). The superior nucleophilicity of Sec, relative to the common 20 amino acids at physiological pH, enables selective modification of antibodies with electrophiles. However, Sec incorporation is limited to the C terminus of proteins (TAG suppression for Sec requires the Sec insertion sequence near the 3′ UTR), thus restricting the variation in potential conjugation sites. Moreover, this approach requires reduction of Sec by reducing agents such as DTT before conjugation, and this reduction can affect multiple disulfide bonds in antibodies and decrease overall yields.

Antibody drug conjugates and bispecific antibodies allow the selective targeting of potent small molecule toxins or cytotoxic T cells to a tumor of interest. Although antibodies can bind to certain target epitopes with high affinity and selectivity, some potential cancer cell-associated antigens, including enzymes, ion channels, G protein-coupled receptors, integrins, and cytokine receptors, also are bound selectively and with high affinity by small molecules. Thus, the ability to target these epitopes with hybrid small molecule ligand–antibody conjugates could be advantageous. In this regard, the small molecule DUPA, which binds to the PSMA active site, coupled to a T cell–recruiting anti-CD3 antibody provides a relevant proof of concept for this small molecule–antibody bispecific format. Indeed P-SMAC is functionally analogous to an antibody with two antigen-binding sites and one effector function. This architecture likely can be generalized to other noncancer targets and effector functions as well. For example, small molecule ligands that can bind specifically to pathogenic bacteria or fungi can be conjugated to Fc receptor-binding antibodies (e.g., anti-CD16b, anti-CD64, anti-

Fig. 4. In vivo efficacy studies of P-SMAC. (A) In the prophylactic model, 1×10^6 C4-2 cells were mixed with 2×10^6 PBMCs (1:2 ratio) in 50% Matrigel and were injected s.c. into the right shoulder of male NOD-SCID mice. P-SMAC, unconjugated Fab, or PBS (vehicle) ($n = 6$) was administered i.v. at 2 mg/kg every day for 10 d starting on day 4. Tumors were monitored by external caliper measurements at regular intervals for 6 wk. P-SMAC suppressed tumor growth, but the control groups rapidly developed tumors. *Mice with large tumors (>1,000 mm³) were killed before the day indicated. (B) In the treatment model, 1×10^6 C4-2 cells with 50% Matrigel were injected s.c. into male NOD/SCID-γ mice. On day 3, 20×10^6 hPBMCs were injected i.p. PBMCs from the same donor were activated ex vivo by incubation with immobilized αCD3 and αCD28 antibodies for 3 d and subsequently were expanded with rh-IL2. Once the solid tumors were palpable (day 13), 20×10^6 activated hPBMCs were injected i.p. Beginning on day 15, 1 mg/kg P-SMAC or PBS was given daily for 10 d i.v. ($n = 9$). (**$P < 0.0001$.)
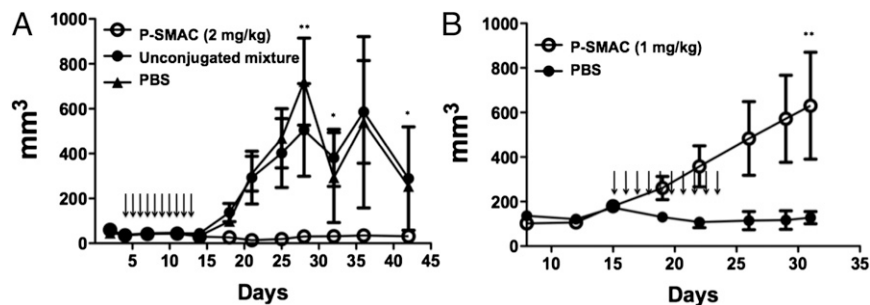
CD89, among others) to recruit specific subsets of immune effector cells such as macrophages and neutrophils for the induction of phagocytosis and microbe killing. Finally, our simple (one-step conjugation and purification) and high-yielding (>90%) semisynthetic approach also is suitable for combinatorial synthesis of diverse bispecific antibodies to screen quickly for optimal combinations of both the target- and effector cell-binding components.

Materials and Methods

For in vitro cytotoxicity assays, PBMCs were purified from fresh healthy human donor blood (from The Scripps Research Institute normal blood donor service) by conventional Ficoll-Hypaque gradient centrifugation (GE Healthcare). Purified PBMCs were washed and incubated in flasks in RPMI medium with 10% (vol/vol) FBS for 1 h to remove any adherent cells. C4-2 (PSMA$^+$) or DU145 (PSMA$^-$) cells (target cells) were dissociated with 0.05% trypsin/EDTA solution (HyClone) and washed with RPMI with 10% (vol/vol) FBS. Then 1×10^4 target cells were mixed with PBMCs at a 1:10 ratio in 100 μL of

RPMI with 10% (vol/vol) FBS and were incubated with different concentrations of conjugated and unconjugated Fabs (10 μL in medium) for 24 h at 37 °C. Cytotoxicity of each well was measured for LDH levels in supernatant using the Cytotox-96 nonradioactive cytotoxicity assay kit (Promega). Lysis solution provided in the same kit (10 μL) was added to wells containing only target cells to achieve the maximum killing, and spontaneous killing was measured in wells with effector and target cells treated with vehicle (10 μL PBS). The absorbance at 490 nm was recorded using a SpectraMax 250 plate reader (Molecular Devices Corp.). Percent cytotoxicity was calculated by:

% cytotoxicity

= (absorbance experimental − absorbance spontaneous average)/

(absorbance maximum killing average − absorbance spontaneous average).

1. American Cancer Society (2012) Cancer Facts and Figures 2012 (American Cancer Society, Atlanta, GA).
2. Nelson WG, De Marzo AM, Isaacs WB (2003) Prostate cancer. N Engl J Med 349(4): 366–381.
3. Kim MM, et al. (2012) Improvement in prostate cancer survival over time: A 20-year analysis. Cancer J 18(1):1–8.
4. Henry MD, et al. (2004) A prostate-specific membrane antigen-targeted monoclonal antibody-chemotherapeutic conjugate designed for the treatment of prostate cancer. Cancer Res 64(21):7995–8001.
5. May KF, Jr., Gulley JL, Drake CG, Dranoff G, Kantoff PW (2011) Prostate cancer immunotherapy. Clin Cancer Res 17(16):5233–5238.
6. Kantoff PW, et al.; IMPACT Study Investigators (2010) Sipuleucel-T immunotherapy for castration-resistant prostate cancer. N Engl J Med 363(5):411–422.
7. Murphy GP, et al. (1999) Infusion of dendritic cells pulsed with HLA-A2-specific prostate-specific membrane antigen peptides: A phase II prostate cancer vaccine trial involving patients with hormone-refractory metastatic disease. Prostate 38(1):73–78.
8. Bühler P, et al. (2009) Target-dependent T-cell activation by coligation with a PSMA x CD3 diabody induces lysis of prostate cancer cells. J Immunother 32(6):565–573.
9. Friedrich M, et al. (2012) Regression of human prostate cancer xenografts in mice by AMG 212/BAY2010112, a novel PSMA/CD3-Bispecific BiTE antibody cross-reactive with non-human primate antigens. Mol Cancer Ther 11(12):2664–2673.
10. Riethmüller G (2012) Symmetry breaking: Bispecific antibodies, the beginnings, and 50 years on. Cancer Immun 12:12.
11. Dannull J, et al. (2000) Prostate stem cell antigen is a promising candidate for immunotherapy of advanced prostate cancer. Cancer Res 60(19):5522–5528.
12. Baeuerle PA, Reinhardt C (2009) Bispecific T-cell engaging antibodies for cancer therapy. Cancer Res 69(12):4941–4944.
13. Sebastian M, et al. (2009) Treatment of malignant pleural effusion with the trifunctional antibody catumaxomab (Removab) (anti-EpCAM x Anti-CD3): Results of a phase 1/2 study. J Immunother 32(2):195–202.
14. Topp MS, et al. (2012) Long-term follow-up of hematologic relapse-free survival in a phase 2 study of blinatumomab in patients with MRD in B-lineage ALL. Blood 120(26):5185–5187.
15. Chames P, Baty D (2009) Bispecific antibodies for cancer therapy: The light at the end of the tunnel? MAbs 1(6):539–547.
16. Graziano RF, Guptill P (2004) Chemical production of bispecific antibodies. Methods Mol Biol 283:71–85.
17. Kim CH, et al. (2012) Synthesis of bispecific antibodies using genetically encoded unnatural amino acids. J Am Chem Soc 134(24):9918–9921.
18. Kularatne SA, Wang K, Santhapuram HKR, Low PS (2009) Prostate-specific membrane antigen targeted imaging and therapy of prostate cancer using a PSMA inhibitor as a homing ligand. Mol Pharm 6(3):780–789.
19. Silver DA, Pellicer I, Fair WR, Heston WD, Cordon-Cardo C (1997) Prostate-specific membrane antigen expression in normal and malignant human tissues. Clin Cancer Res 3(1):81–85.
20. Milowsky MI, et al. (2004) Phase I trial of yttrium-90-labeled anti-prostate-specific membrane antigen monoclonal antibody J591 for androgen-independent prostate cancer. J Clin Oncol 22(13):2522–2531.
21. Kuroda K, et al. (2010) Saporin toxin-conjugated monoclonal antibody targeting prostate-specific membrane antigen has potent anticancer activity. Prostate 70(12): 1286–1294.
22. Zhou J, Neale JH, Pomper MG, Kozikowski AP (2005) NAAG peptidase inhibitors and their potential for diagnosis and therapy. Nat Rev Drug Discov 4(12):1015–1026.
23. Chen Y, et al. (2008) Radiohalogenated prostate-specific membrane antigen (PSMA)-based ureas as imaging agents for prostate cancer. J Med Chem 51(24):7933–7943.
24. Krall N, Scheuermann J, Neri D (2013) Small targeted cytotoxics: Current state and promises from DNA-encoded chemical libraries. Angew Chem Int Ed Engl 52(5): 1384–1402.
25. Zhang AX, et al. (2010) A remote arene-binding site on prostate specific membrane antigen revealed by antibody-recruiting small molecules. J Am Chem Soc 132(36): 12711–12716.
26. Zhu Z, Carter P (1995) Identification of heavy chain residues in a humanized anti-CD3 antibody important for efficient antigen binding and T cell activation. J Immunol 155(4):1903–1910.
27. Wang L, Zhang Z, Brock A, Schultz PG (2003) Addition of the keto functional group to the genetic code of Escherichia coli. Proc Natl Acad Sci USA 100(1):56–61.
28. Shalaby MR, et al. (1992) Development of humanized bispecific antibodies reactive with cytotoxic lymphocytes and tumor cells overexpressing the HER2 protooncogene. J Exp Med 175(1):217–225.
29. Cho H-S, et al. (2003) Structure of the extracellular region of HER2 alone and in complex with the Herceptin Fab. Nature 421(6924):756–760.
30. Chatterjee A, Sun SB, Furman JL, Xiao H, Schultz PG (2013) A versatile platform for single- and multiple-unnatural amino acid mutagenesis in Escherichia coli. Biochemistry 52(10):1828–1837.
31. Murelli RP, Zhang AX, Michel J, Jorgensen WL, Spiegel DA (2009) Chemical control over immune recognition: A class of antibody-recruiting small molecules that target prostate cancer. J Am Chem Soc 131(47):17090–17092.
32. Hutchins BM, et al. (2011) Site-specific coupling and sterically controlled formation of multimeric antibody fab fragments with unnatural amino acids. J Mol Biol 406(4): 595–603.
33. McCall AM, et al. (2001) Increasing the affinity for tumor antigen enhances bispecific antibody cytotoxicity. J Immunol 166(10):6112–6117.
34. Davis MI, Bennett MJ, Thomas LM, Bjorkman PJ (2005) Crystal structure of prostate-specific membrane antigen, a tumor marker and peptidase. Proc Natl Acad Sci USA 102(17):5981–5986.
35. Park BK, Kitteringham NR (1990) Drug-protein conjugation and its immunological consequences. Drug Metab Rev 22(1):87–144.
36. Decker T, Lohmann-Matthes ML (1988) A quick and simple method for the quantitation of lactate dehydrogenase release in measurements of cellular cytotoxicity and tumor necrosis factor (TNF) activity. J Immunol Methods 115(1):61–69.
37. Haas C, et al. (2009) Mode of cytotoxic action of T cell-engaging BiTE antibody MT110. Immunobiology 214(6):441–453.
38. Kurtzhals P, et al. (1995) Albumin binding of insulins acylated with fatty acids: Characterization of the ligand-protein interaction and correlation between binding affinity and timing of the insulin effect in vivo. Biochem J 312(Pt 3):725–731.
39. Chapman AP, et al. (1999) Therapeutic antibody fragments with prolonged in vivo half-lives. Nat Biotechnol 17(8):780–783.
40. Klinger M, et al. (2012) Immunopharmacologic response of patients with B-lineage acute lymphoblastic leukemia to continuous infusion of T cell-engaging CD19/CD3-bispecific BiTE antibody blinatumomab. Blood 119(26):6226–6233.
41. Janda KD, Treweek JB (2012) Vaccines targeting drugs of abuse: Is the glass half-empty or half-full? Nat Rev Immunol 12(1):67–72.
42. Yan L, Ehrlich PJ, Gibson R, Pickett C, Beckman RA (2009) How can we improve antibody-based cancer therapy? MAbs 1(1):67–70.
43. Cui HT, Thomas JD, Burke TR, Jr., Rader C (2012) Chemically programmed bispecific antibodies that recruit and activate T cells. J Biol Chem 287(34):28206–28214.